

Black Carbon Particulate Matter Emission Factors for Buoyancy Driven Associated Gas Flares

James D.N. McEwen and Matthew R. Johnson*

Energy and Emissions Research Lab, Mechanical & Aerospace Engineering,
Carleton University, Ottawa, ON, Canada, K1S 5B6

This is a preprint of an article whose final and definitive form has been published in the Journal of the Air & Waste Management Association © 2012 Taylor & Francis. The final published article can be cited as: J.D.N. McEwen & M.R. Johnson, Black carbon particulate matter emission factors for buoyancy driven associated gas flares J. Air Waste Manage. Assoc., 62(3):307-321 (doi: 10.1080/10473289.2011.650040) and is available online at <http://www.tandfonline.com/openurl?genre=article&issn=1096-2247&volume=62&issue=3&spage=307>.

*Corresponding Author: Email: Matthew_Johnson@carleton.ca; 613 520 2600 ext. 4039

ABSTRACT

Flaring is a technique used extensively in the oil and gas industry to burn unwanted flammable gases. Oxidation of the gas can preclude emissions of methane (a potent greenhouse gas); however flaring creates other pollutant emissions such as particulate matter (PM) in the form of soot or black carbon (BC). Currently available PM emission factors for flares were reviewed and found to be questionably accurate, or based on measurements not directly relevant to open-atmosphere flares. In addition, most previous studies of soot emissions from turbulent diffusion flames considered alkene or alkyne based gaseous fuels, and few considered mixed fuels in detail and/or lower sooting propensity fuels such as methane, which is the predominant constituent of gas flared in the upstream oil and gas industry. Quantitative emission measurements were performed on lab-scale flares for a range of burner diameters, exit velocities, and fuel compositions. Drawing from established standards, a sampling protocol was developed that employed both gravimetric analysis of filter samples and real-time measurements of soot volume fraction using a Laser Induced Incandescence (LII) system. For the full range of conditions tested (burner inner diameter (ID) of 12.7-76.2 mm, exit velocity 0.1-2.2 m/s, 4- and 6-component methane-based fuel mixtures representative of associated gas in the upstream oil industry), measured soot emission factors were less than 0.84 kg soot/10³ m³ fuel. A simple empirical relationship is presented to estimate the PM emission factor as a function of the fuel heating value for a range of conditions, which although still limited, is an improvement over currently available emission factors.

IMPLICATIONS

Despite the very significant volumes of gas flared globally and the requirement to report associated emissions in many jurisdictions of the world, a review of the very few existing particulate matter emission factors has revealed serious shortcomings sufficient to suggest that estimates of soot production from flares based on current emission factors should be interpreted with caution. New BC emissions data are presented for lab-scale flares in what are believed to be the first such experiments to consider fuel mixtures relevant to associated gas compositions. The empirical model developed from these data is an important step toward being able to better predict and manage BC emissions from flaring.

INTRODUCTION

Flaring is the common practice of burning off unwanted, flammable gases via combustion in an open-atmosphere, non-premixed flame. This gas may be deemed uneconomic to process (i.e. if it is far from a gas pipeline or if it is 'sour' and contains trace amounts of toxic H₂S) or it may occur due to leakages, purges, or an emergency release of gas in a facility. Estimates derived from satellite imagery suggest more than 139 billion cubic meters of gas were flared globally in 2008.¹ While the composition of flared gas can vary significantly, within the upstream oil and gas (UOG) industry, generally, the major constituent is methane. Since methane has a 25 times higher Global Warming Potential (GWP) (on a 100 year time-scale) than CO₂ on a mass basis,² flaring can preclude significant greenhouse gas emissions that would occur if the gas were simply vented into the atmosphere. However, flaring can produce soot and other pollutant species that have negative effects on air quality and the environment.³⁻⁶ Soot is implicated as a significant health hazard primarily because of its small size,⁷ and it has been linked to serious, adverse cardiovascular, respiratory, reproductive, and developmental effects in humans.⁸ Soot has also been recognized as an important source of anthropogenic radiative forcing of the planet's surface.^{2,9,10} The key objectives of this paper are to review and critically assess current understanding of soot emissions from flares typical of the upstream oil and gas industry, and to present results of experiments aimed at developing a better methodology for accurately predicting these critical emissions.

Estimates of emissions from flaring are complicated by the large diversity of flare designs, applications, and operating conditions encountered. Industrial flares may be broadly classed as emergency flares, process flares, or production flares.^{11,12} Emergency flaring is by

definition intermittent and typically involves large, very short duration, unplanned releases of flammable gas that is combusted for safety reasons. Flare stack exit velocities during emergency flaring can approach sonic. Process flaring may involve large or small releases of gas over durations ranging from hours to days, as is encountered in the upstream oil and gas industry during well testing to evaluate the size of a reservoir, or at downstream facilities during blow-down or evacuation of tanks and equipment. Production flaring typically involves smaller, more consistent gas volumes and much longer durations that may extend indefinitely during oil production, in situations where associated gas (a.k.a. solution gas) is not being conserved. The design of a flare can also vary significantly, ranging from simple pipe flares (essentially an open-ended vertical pipe) that are common in the UOG industry, to flares with engineered flare tips that can include multiple fuel nozzles and multipoint air and/or steam injection for smoke suppression.¹² In terms of emissions, key factors that can affect flare performance include the exit velocity of gas from the flare, the flare gas composition, ambient wind conditions, flare stack diameter, and flare tip design.^{5,13}

Previous Emissions Measurements from Flares

Despite the ubiquity of flares in the world, there have been relatively few successful studies investigating their emissions,^{3-6,13-17} and most have focused on quantifying gas-phase carbon conversion efficiencies. Progress has been hampered by the inherent difficulties in accurately sampling emissions from an unconfined, turbulent, inhomogeneous, elevated plume of a flare. General understanding is further complicated by the incredibly wide range of operating conditions (i.e. exit velocities, cross-wind conditions, fuel compositions) encountered in different applications. For pilot-

scale flares in the absence of crossflow, both Pohl⁴ and Seigel¹⁷ traversed a sample probe above the flare and found gas phase carbon conversions efficiencies in excess of 98%, except at low heating values near the limits of flame stability.⁴ Although Siegel attempted to consider effects of moderate crosswinds using a blower system, because of problems measuring velocities in the unsteady plume, he was only able to report “local” conversion efficiencies based on ratios of gas-phase species concentrations at the location of the sample probe. Nevertheless, for the high hydrogen flare gas mixture (54.5% H₂, 42.8% C₁-C₆ hydrocarbons) considered by Seigel, he found local efficiencies typically above 95% in low-moderate crosswinds up to ~5 m/s. These results stand in contrast to single-point field measurements by Strosher^{3,18} taken downstream of two “solution gas” flares (i.e. low-exit-velocity flares at upstream oil production facilities burning gas released from solution when produced oil is brought to the surface). Strosher found local efficiencies (calculated to include carbon emissions from the flare) ranging from 62%-84% downstream of the flame tip and suggested that these lower efficiencies might be linked to carry-over of liquids into the flare gas stream. However, it has been shown for both pilot-scale vertical flares,⁴ and lab-scale flares in crossflow,^{19,20} that the composition of the product plume is inhomogeneous, which presents a significant challenge in interpreting efficiency measurements derived from single-point samples of the plume. Pohl et al.⁴ showed that the fraction of unburned hydrocarbons could vary by more than a factor of two across the plume.

Apart from the few known pilot-scale studies cited above, most general understanding of the factors affecting flare emissions has been derived from wind tunnel testing of lab-scale flares under controlled conditions. Data from experiments in a closed-loop wind tunnel where

the entire plume of products from the flare could be captured,^{5,6,13,21} have shown that in the case of low-exit velocity (~0.5-5 m/s) pipe flares burning hydrocarbon fuels mixtures with heating values equal to or greater than that of natural gas (~37 MJ/m³), gas phase efficiencies above 98-99% could be expected at low-crosswind speeds. However, efficiencies reduced rapidly at high crosswind speeds, with a functional dependence that varied with $U_{\infty}/(V_j^{1/3})$, where U_{∞} is the crosswind velocity and V_j is the exit velocity of the flare gas. Inefficiencies under these conditions were primarily in the form of unburned fuel driven by a coherent-structure based fuel stripping mechanism.^{6,22} Experiments also revealed that quite low efficiencies at flare gas heating values below ~20 MJ/m³,^{5,13,15} which was the impetus for regulatory changes to the minimum permissible flare gas heating value in the Province of Alberta, Canada.²³ A crude parametric model was proposed for low-momentum, hydrocarbon pipe-flares in crossflow based on these results,¹³ however because of the empiricism in the model, it is limited to the range of conditions considered in the experiments.

Previous Measurements of Soot Emissions from Flares. In one of the few works to consider soot emissions from flares, McDaniel²⁴ collected soot samples on filters for gravimetric analysis using a single-point probe suspended above a 203.2 mm diameter pilot-scale flare burning “crude propylene” (approximately 80% propylene, 20% propane) with exit velocities from 2.3-4.2 m/s. The typical flare in McDaniel²⁴ used steam for smoke suppression during experiments to measure combustion efficiency. However, for the conditions where soot was measured, the steam flow was disabled to purposefully produce a smoking flare. The soot measurements made in this work were

reported in terms of exhaust gas soot concentration only, and since the dilution of the samples was not known, data were not directly relatable to fuel consumption as is standard with emissions factors.

Pohl et al.⁴ investigated the effect of soot on combustion efficiency from pilot-scale flares burning propane with burner diameters ranging from 76.2 mm to 304.8 mm and exit velocities ranging from 0.03 m/s to 30 m/s. Soot was captured on a “filter at the end of a probe, and its concentration [was] determined by burning combustibles from the filter.”⁴ While soot concentrations or emission rate data were not directly reported, the authors concluded that soot emissions accounted for “less than 0.5 percent of the combustion inefficiencies for most of the conditions tested.”⁴

In the only other known study to specifically consider soot emissions from a flare, the Ph.D. thesis of Siegel¹⁷ attempted to indirectly quantify soot emissions as the residual carbon from a mass balance on measurable gas phase carbon containing species. The pilot flare in the tests of Siegel used a commercial flare tip with a diameter of 700 mm burning a refinery relief gas mixture with exit velocities from 0.1 to 2.5 m/s. The refinery relief gas mixture had a high concentration of hydrogen (55% on average) and would be expected to produce less soot upon stable operation. Although Siegel was able to conclude that in the absence of crosswind, the gas-phases efficiencies were unchanged by the presence of visible soot emission, the uncertainties in closing the carbon mass balance were too high to reliably estimate soot emissions themselves. In one particular test, four single point filter samples of soot were taken above the flare but measured concentrations varied by a factor of 3.5, and Siegel cautioned that it was impossible to specify an emission factor for soot in a flare and his results should be used as reference only (quoted in German as: “Es sei

aber nochmals darauf hingewiesen, dass die Angabe eines Emissionsfaktors für Ruß bei Fackelflammen nicht möglich ist und dass die hier aufgeführten Werte als Orientierung und nicht als bindend gewertet werden sollten.”¹⁷).

Recently, a new technique for directly measuring mass flux of soot from visibly sooting flares under field conditions has been demonstrated.^{25,26} Although this approach has promise as a potential monitoring technique for flare emissions, it is still under development. To date the technique has only been applied to a single, large, visibly-sooting flare for which emissions of 2.0 ± 0.66 g/s were measured; approximately equivalent to “soot emissions of ~500 buses constantly driving.”²⁶

None of the studies cited above specifically considered the effects of crosswind on soot emissions. Increased wind speeds have been shown to reduce the overall combustion efficiency of flares,^{5,6,13,15} however limited available data suggest that the increased mixing of ambient air can slightly decrease the amount of soot produced.¹⁵ This observation is consistent with the only other known study in this regard,²⁷ which examined small-scale (1.04 mm to 2.16 mm diameter) propane diffusion flames under cross-flow and co-flow conditions. The current research focuses on the quiescent wind conditions only (i.e. zero cross-flow), which should represent the “worst case” sooting scenario.

CURRENT PM_{2.5} EMISSION FACTORS

Given the state of knowledge and lack of available models to predict soot emissions from flares, it is worth briefly examining how emission estimates for pollutant inventories and regulatory decisions are currently derived. In most developed jurisdictions throughout the world, key pollutants such as particulate matter less than 2.5 μm in diameter (PM_{2.5}), which includes soot from flares, must be reported and

are tracked in government emissions inventories. Emissions are generally estimated using simple emission factors that specify a unit of pollutant emitted per unit of fuel consumed. Given the wide variation in flare emissions associated with large variations in meteorological conditions, fuel composition, fuel flow rates, flare size, and flare design, this approach to estimating emissions is at best overly simplified.

Existing PM_{2.5} emission factors for flares are essentially limited to three sets of values published in the US EPA WebFIRE database,²⁸ as summarized in Table 1 and converted to common units for comparison. These include a factor from a confidential report based on landfill gas flares,²⁹ a factor from AP-42 section 2.4³⁰ from landfill gas flares, and a factor from AP-42 section 13.5³¹ from industrial flares. Emission factors in other jurisdictions (e.g. Canada) are typically based on these data due to the general lack of measurements available on PM_{2.5} from flares. For the UOG industry in Canada, the Canadian Association of Petroleum

Producers (CAPP) has produced a guide³² to help industry members report their emissions to the National Pollutant Release Inventory (NPRI) as required. The emission factor used to estimate production of soot from flares in Canada (also shown in Table 1) is derived from the emission factor attributed to the confidential report from the US EPA entitled “Data from flaring landfill gas.”²⁹ This emission factor is published in US EPA’s WebFIRE database as 0.85 kg soot per 10³ m³ of fuel.²⁸ The CAPP guide instead gives a value of 2.5632 kg soot per 10³ m³ of fuel and notes that the US EPA value has been “corrected” for a gas with a heating value of 45 MJ/m³. The CAPP guide does not specify how this apparent factor of three correction was derived, although it likely resulted from an assumed linear scaling of soot emission with heating value, since landfill gas could be expected to have a heating value on the order of 15 MJ/m³, and a heating value of 45 MJ/m³ should be typical of flare gas in the UOG industry.

Table 1: Comparison of Current Soot Emission Factors for Flares

Standard	Original Emission Factor	EF (kg PM per 10 ³ m ³ of fuel)	Fuel Gas
USEPA FIRE 6.25 ²⁸	53 lb PM per 10 ⁶ ft ³ gas	0.85	Landfill Gas ^a
	17 lb PM per 10 ⁶ ft ³ gas	0.27	Methane
	0, 40, 177, 274 lb PM per 10 ⁶ BTU	0, 1500, 6634, 10270 ^b	80% Propylene 20% Propane
CAPP Guide ³²	2.5632 kg PM per 10 ³ m ³ fuel	2.5632	Associated Gas
USEPA AP-42 Vol. I, section 13.5 ³¹	0, 40, 177, 274 ^c µg PM per 10 ⁻³ m ³ exhaust gas	0, 0.9, 4.2, 6.4 ^d	80% Propylene 20% Propane

^a While the source for this emission factor is not publicly available and the composition of landfill gas varies, a typical composition could be 56% methane, 37% CO₂, 1% O₂, and trace amounts of other gasses.⁵⁸

^b Based on a fuel heating value of 87 MJ/m³ (1 BTU = 1055.06 J).

^c The four different values are based on the “smoking level” of the flare: non-smoking flares, 0 µg/L; lightly smoking flares, 40 µg/L; average smoking flares, 177 µg/L; and heavily smoking flares, 274 µg/L.³¹

^d These emission factors were calculated by the present authors from the original reported exhaust gas emission factors, assuming no dilution and simple combustion chemistry.

As can be seen in Table 1, the emission factors vary by orders of magnitude. Of the three different factors for flares reported in US EPA's WebFIRE,²⁸ the first two were largely derived from measurements on enclosed flares (although full details of the measurements are not publicly available), while burning gas compositions (pure methane and landfill gas) that would have limited relevance to UOG flares. The third factor, as reported, is up to 5 orders of magnitude higher than the other two values. However, quite significantly, a review of the source data for this factor reveals an apparent clerical error in the form of a swap of units from $\mu\text{g PM per } 10^{-3} \text{ m}^3 \text{ exhaust gas}$ to $\text{lb PM per } 10^6 \text{ BTU}$, between the emission factor as reported in US EPA AP-42³¹ and the value reported in US EPA WebFIRE;²⁸ both are attributed to the same data source.²⁴ This error was formally reported to US EPA and has been corrected in the US EPA's draft review document "Emissions Estimation Protocol for Petroleum Refineries (v.2.0)".

Irrespective of reporting errors in these data, none of these factors is based on measurements from actual associated gas flares typical of the UOG industry (the CAPP guide value is derived from the US EPA value), and none gives any consideration to operating conditions of a flare including wind speed, exit velocity, detailed fuel composition, flare size, or flare tip design, even though these parameters can significantly affect soot production. These discrepancies and simplifications bring into question the validity and credibility of the emission factors used for the significant global volumes of flared gas. The lack of accurate guidelines for estimating and reporting of soot from flares in the UOG industry is the primary motivation for the current work.

THE FLARE AS A VERTICAL DIFFUSION FLAME

Flares are elevated turbulent jet-diffusion flames. Jet-diffusion flames subjected to cross-flowing winds may be broadly categorized into two groups based on the momentum flux ratio, $R = \rho_j u_j^2 / (\rho_\infty u_\infty^2)$, where ρ is density, u is velocity, and the subscript j and ∞ denote the jet and cross-flow fluid respectively [e.g. ^{5,33,34}]. At high momentum flux ratios, the strength of the jet dominates, and the effects of the cross-wind are relatively unimportant.³³ At low momentum flux ratios, the flame bends over significantly in the wind and, at very low momentum flux ratios, the flame can be drawn down below the jet exit plane and become "wake-stabilized" on the leeward side of the stack [e.g. ^{5,6,34}].

Flares in quiescent wind conditions (i.e. high R) may be further categorized depending on whether the flame behavior is dominated by buoyancy of the hot gases or momentum of the reactants. Several studies on turbulent diffusion flames make use of a flame or fuel derived Froude number, Fr , to define the flame regime as momentum or buoyancy driven.³⁵⁻³⁷ Delichatsios³⁷ has elaborated on this notion to define a regime map for vertical turbulent diffusion flames, in which different flame regimes are defined depending on whether the turbulence is generated by instabilities present in the cold flow, or by the large buoyancy forces present in the flame. The "type" of turbulence generated will depend on the magnitude of the buoyancy forces to the inertia forces in the flame. Delichatsios³⁷ has identified these regimes as well as other sub-regimes based on the mode of transition from laminar to turbulent, in a graphical form as is shown in Figure 1. The main regimes of interest in the current work are the "turbulent-buoyant transition-buoyant" and "turbulent-buoyant transition-shear" regimes. It should be noted that the transitions between regimes are expected to be smooth, so that the

dashed lines in Figure 1 should not represent a sudden change. The vertical axis of Figure 1 is simply the source Reynolds number based on the fuel properties, and the horizontal axis of Figure 1 is the fuel gas Froude number (Fr_g) (termed the modified fire Froude number by Delichatsios³⁷), defined as shown in eq 1.

$$Fr_g = \frac{u_e f_s^{3/2}}{(gd_e)^{1/2} (\rho_e / \rho_\infty)^{1/4}} \quad (1)$$

where u_e is the exit velocity [m/s], f_s is the stoichiometric mixture fraction, g is the gravitational acceleration [m/s^2], d_e is the burner exit diameter [m], ρ_∞ is the ambient density [kg/m^3], and ρ_e is the fuel density [kg/m^3].

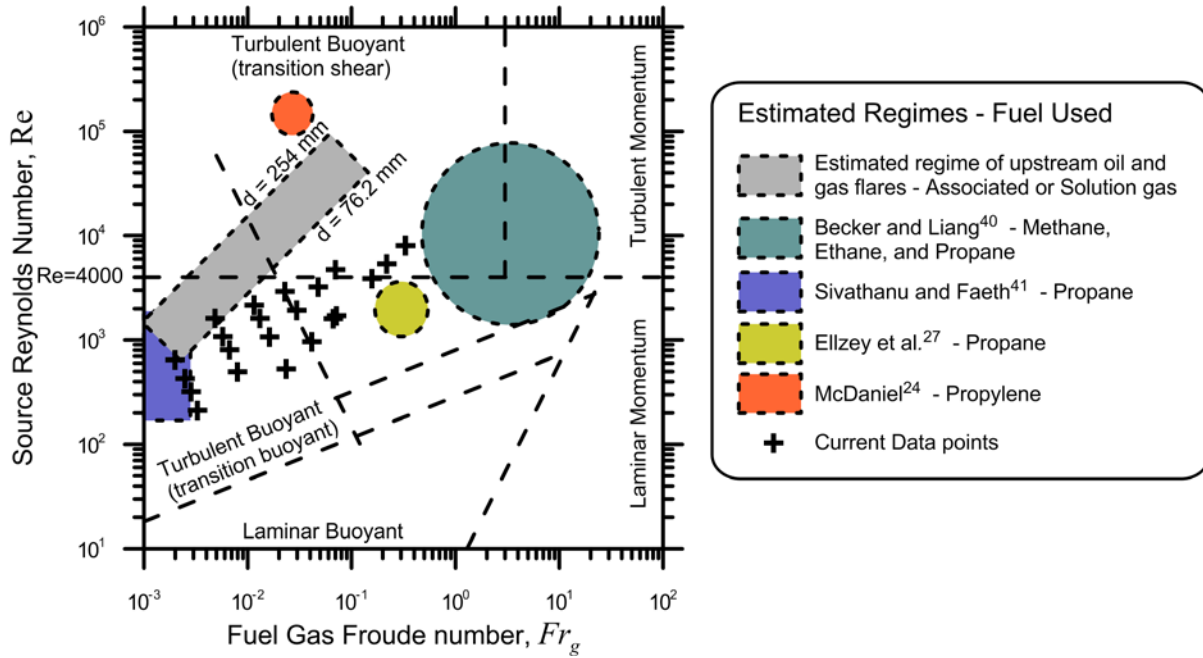


Figure 1: Regime map of turbulent jet-diffusion flames as proposed by Delichatsios³⁷ shown with relevant currently available soot emission measurement conditions from the literature. Shaded areas represent the estimated limits of test/operating conditions, rather than actual test points. The shaded inclined rectangle represents the expected operating regime of buoyancy driven flares typical of the upstream oil and gas industry, with diameters ranging from 76.2 mm to 254 mm as shown, and exit velocities of 0.1 m/s (values in the lower left of the shaded region) to 6 m/s (values in the upper right).

For continuous flares used to dispose of associated gas (a.k.a. solution gas) in the upstream oil and gas industry, an estimated range of expected conditions is identified by the inclined shaded rectangle in Figure 1. These conditions were calculated based on typical associated gas flares for Alberta, Canada,^{11,38} where the bounding lower line represents a 76.2 mm burner and the upper line represents the 254 mm burner, and exit velocities span a range of 0.1 to 6 m/s. According to the theory of

Delichatsios³⁷, this range of flame conditions could all be classified as turbulent-buoyant, although they span both the transition-buoyant, and transition-shear sub-regimes. This information was used in determining flow conditions in an attempt to span both sub-regimes under the assumption that the sub-regime of the flame may impact the soot yield.

Previous Studies of Soot Emissions from Turbulent Diffusion Flames

Total soot emission from turbulent diffusion flames has been studied in the past.³⁹⁻⁴¹

However, these works typically considered pure fuels comprised of heavier sooting alkene or alkyne hydrocarbons. Where alkanes have been studied, typically only propane has been considered. Becker and Liang⁴⁰ studied soot emissions from the alkane family of fuels more thoroughly however, and to the authors' knowledge, their data are the only measurements of the total soot emission in the literature to include data from methane, ethane, and propane diffusion flames. Although they were not able to develop a theory for scaling soot emissions, they were able to demonstrate that the soot emission changed under varying flow conditions (i.e. burner size, exit velocity, fuel). The different flow conditions were identified by a Richardson ratio (Ri_L), as defined in eq 2.

$$Ri_L = \frac{gL_f^3}{(u_e d_e)^2} \left(\frac{\rho_\infty}{\rho_e} \right) \quad (2)$$

where L_f is the flame length [m]. As can be seen, there is a heavy dependence of Ri_L on the flame length, and if flame length values vary slightly, large discrepancies in calculated Ri_L values can appear. Because the length of a turbulent flame is an ill-defined quantity, this flame length term is somewhat undesirable in terms of its sensitivity.

The work of Sivathanu and Faeth⁴¹ with propane also showed that soot emission varied with flow conditions, and proposed simple correlations of the measured soot emission with a smoke-point normalized residence time, $\bar{\tau}_{sp} = \tau_R / \tau_{sp}$ (where τ_R is the measured residence time and τ_{sp} is the measured smoke-point residence time). The smoke-point of a fuel is an experimentally

derived parameter that allows for comparisons of the sooting tendency between different fuels. Sivathanu and Faeth⁴¹ had defined residence time as the time interval between the interruption of the fuel flow (via a shutter that rapidly closed over the burner exit), and the disappearance of all flame luminosity.

Both these works highlight the fact that soot emission changes with flow conditions and fuel, and a single emission factor applied to all conditions may be inappropriate. A comparison of these data, created by digitization of selected available raw data plots and shown in Figure 2, reveals further challenges. Specifically, the variation in soot yields spans several orders of magnitude necessitating the use of a log scale to display the data. More curiously, while the data of Sivathanu and Faeth⁴¹ show the anticipated sensitivity of soot yield to fuel composition, the data of Becker and Liang⁴⁰ suggest that in the range of $Fr_g \approx 5$, the soot yields of methane, ethane, propane, and ethylene essentially overlap. The agreement between corresponding data sets of the two authors is not especially strong, especially for acetylene where the flow conditions appear to be similar (i.e. $Fr_g \approx 10$) and soot yields vary by a factor of 4-8 or more. The present data for methane similarly do not align with data of Becker and Liang⁴⁰, although the comparable experiments were at significantly different Froude numbers as indicated on the plot. In general, Figure 2 serves to show that where limited comparable data do exist for multiple flow conditions and fuels, there are still discrepancies. However, this may partially be attributed to that the fact that the Froude number in the work of Becker and Liang was calculated from the reported Richardson ratio, which could be expected to have a large variation based on the subjectivity of the flame length measurement.

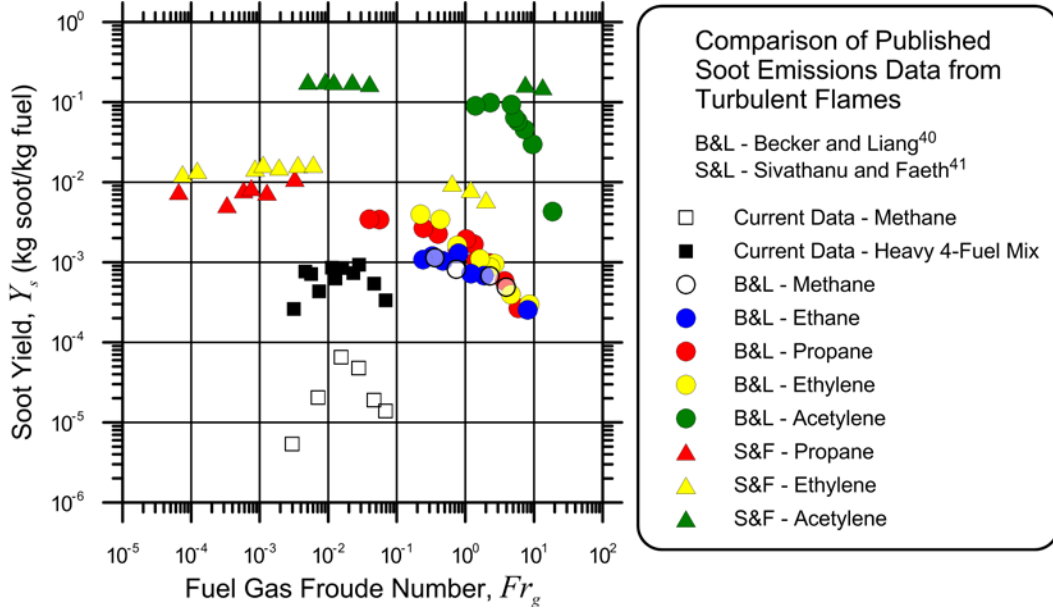


Figure 2: Comparison of soot emission measurements from Becker and Liang,⁴⁰ Sivathanu and Faeth,⁴¹ and current measurements using pure methane and the heavy four-component fuel mix.

In another work of Delichatsios,³⁹ simple soot emission measurements were made for several fuels, including propane, and a reasonable correlation for the scaling of soot yield with a calculated smoke-point heat release rate and stoichiometric ratio was presented, as shown in eq 3. The smoke-point heat release rate was calculated according to eq 4.

$$Y_s \sim \dot{S}_{sp} f_s \quad (3)$$

$$\dot{S}_{sp} = \dot{m}_{fuel,sp} \Delta H_c \quad (4)$$

where $\dot{m}_{fuel,sp}$ is the mass flow rate at the smoke-point and ΔH_c is the heat of combustion. While the heat release is an easy parameter to monitor, the smoke-point heat release is difficult to calculate for multi-component fuel mixtures. Compounding this problem is the lack of measurements of the smoke-point for methane, since the flame becomes unstable before it starts to smoke in a standard smoke-point measurement test.⁴²

Glassman⁴³ suggested that the flame temperature and length of time that soot particles reside at

these elevated temperatures have a direct effect on the soot formation. Glassman postulated that what controls the soot volume fraction that exits the flame and causes soot emission is the distance between the isotherms that specify the incipient particle formation temperature and stoichiometric flame temperature (indicative of the strength of the temperature gradient). This distance establishes the growth time of the particles formed before flame oxidation of the soot occurs.⁴³ While a universal theory for soot emission as a function of some temperature parameter is not given, it highlights the importance of the flame temperature on the soot formation.

Finally, Ouf et al.⁴⁴ presented data on the effects of over-ventilating the flame on soot emissions. Specifically they were interested in changes in the size distributions of the primary particles and soot aggregates, morphology, and soot emission as a function of the global equivalence ratio. Specifically, Ouf et al. found that the global equivalence ratio strongly influences the soot particle size, but does not play a predominant

role in other soot morphological properties or emission rates.⁴⁴

In short, a thorough review of the published literature on soot emissions of flares and vertical diffusion flames has revealed very little data that is directly relevant to the anticipated flow regimes and fuel compositions of flares typical of the upstream oil and gas industry.

Furthermore, although a few different scaling parameters have been suggested, agreement among the limited comparable data currently available are generally poor. The controlled lab-scale experiments presented below provide new insight into this complex problem and represent important first steps toward developing practical models to predict soot emissions from flares.

EXPERIMENTAL METHODS

Experiments were conducted in a Lab-Scale Flare (LSF) facility, which consists of a vertical

turbulent jet-diffusion burner and hooded sampling system as shown schematically in Figure 3. Fuel mixtures consisting of any or all of CH_4 , C_2H_6 , C_3H_8 , C_4H_{10} , CO_2 , and N_2 could be metered, mixed, delivered to the burner at fuel flow rates of up to 100 SLPM, and ejected from flare tips with exit diameters of 12.7, 25.4, 38.1, 50.8, or 76.2 mm. The entire combustion product plume and additional entrained room air were collected via a hood and drawn into a 152.4 mm diameter insulated dilution tunnel (DT), which was vented to the atmosphere with a variable speed exhaust fan. Emissions were drawn from the DT and samples were collected on filters for later gravimetric analysis or routed directly to a Laser Induced Incandescence system (LII, Artium Technologies Inc., LII200) for concentration measurement. Both data sets were used to calculate the total soot emission rates.

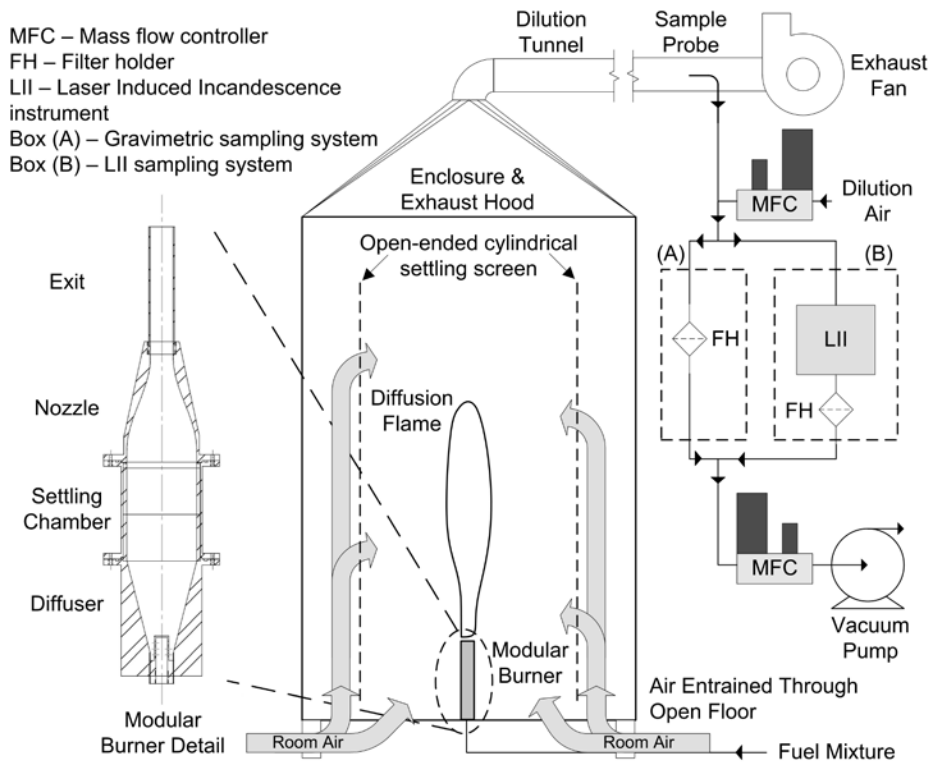


Figure 3: Schematic diagram of the lab-scale flare system. Modular burner detail shown with 25.4 mm I.D. exit and nozzle.

Fuel Mixture Compositions

Up to six separate components of the fuel mixtures (4 hydrocarbons and 2 inerts) were chosen based on the analysis of data from associated gas samples at 2908 distinct upstream oil production sites in Alberta. These data were received as a private communication through the technical steering committee of the Petroleum Technology Alliance of Canada (PTAC), specifically to support this work (private communication between PTAC and M.R. Johnson, 2007). Analysis of these data has shown that methane is the major constituent of the gases being flared. To reduce the complexity of the experiment, surrogate mixtures were used based on the six most abundant components (i.e. mixtures of C1-C4, CO₂, and N₂). Higher hydrocarbons C5 through C7, He, and H₂ were not included in the test mixtures due to their very low concentrations. Thus, results of these experiments are primarily relevant to lighter hydrocarbon flare gas mixtures, which could be expected in upstream oil and gas flares with functioning liquid knockout systems.⁴⁵ Hydrogen sulphide, H₂S, was also neglected primarily due to its extreme toxicity, but also because it was absent from most fuel mixtures (a.k.a. sweet gas). Although detailed speciation of hydrocarbon components

was not available in the provided data, typical components in natural gas from both dry and wet reservoirs are alkane based.⁴⁶ Furthermore, results from a limited sampling of six operating flares in Alberta have also confirmed that the principle hydrocarbons were all alkane based.⁴⁵ Thus, in the present work the hydrocarbon fuel species C1 through C4 were assumed to be alkanes.

Average surrogate test mixtures of flare gas were created by scaling selected component concentrations by their concentrations in the full mixture. Lighter and heavier fuel mixtures were also created (Table 2) to investigate the effects of fuel composition on soot yield. To create the light mixture, the 90th percentile methane concentration was chosen as an upper bound, and the remaining fuel concentrations were determined based on their relative concentrations in the average fuel mixture (i.e. propane to ethane ratio constant, etc.). The heavy mixture was created in the same manner except that the 10th percentile methane concentration was chosen as a lower bound. The same process was repeated neglecting the diluents of CO₂ and N₂ to create 4-component fuel mixtures. The concentrations of all surrogate gas mixtures used in this study are summarized in Table 2.

Table 2: Average, light, and heavy four- and six-component fuel mixtures

Species	Gas Purity (%)	Average Mixture (%)		Light Mixture (%)		Heavy Mixture (%)	
		6-Mix	4-Mix	6-Mix	4-Mix	6-Mix	4-Mix
Methane	99.0	85.24	88.01	91.14	91.14	74.54	74.54
Ethane	99.0	7.06	7.28	4.23	5.38	12.17	15.47
Propane	99.0	3.11	3.21	1.87	2.38	5.37	6.83
n-Butane	99.0	1.44	1.5	0.87	1.1	2.49	3.16
CO ₂	99.99	1.91	0	1.14	0	3.28	0
N ₂	99.999	1.24	0	0.75	0	2.15	0

Enclosure and Emission Collection System

The LSF enclosure was initially developed in the work of Canteenwalla,⁴⁷ and was designed based on the work of Sivathanu and Faeth.⁴¹ The LSF burner is centered inside the 1.5 x 1.5 by 2.6 m tall sheet metal protective enclosure that sits 50 mm above the floor to allow easy air entrainment. A 1 m diameter, 2 m high mesh (690 wires/m, 0.23 mm wire diameter), open-ended cylindrical screen surrounds the flame to prevent buffeting of the flame from room currents. The front of the enclosure has two doors, one made of steel sheet metal, and the other of plexi-glass to provide visual access to the LSF. The top of the enclosure contracts and directs the entire exhaust plume and entrained dilution air into a 152.4 mm ID insulated, galvanized steel pipe. The 152.4 mm pipe acts as a dilution tunnel in which the combustion products and entrained room air are drawn by the exhaust fan and mixed prior to being sampled, as shown in Figure 3. The entrained room air was not separately filtered; however measurements performed drawing samples from the system without the flame ignited showed that whatever particles were contained in the room air fell below detectable limits. The flow of diluted exhaust was assisted by an industrial centrifugal fan capable of drawing 13,000 LPM through the DT and controlled using a variable speed motor and controller. Calculations have shown⁴⁷ that once the system is warmed up to stable operating conditions, deposition of soot on the DT walls or sample line walls is negligible.

To establish a consistent, reliable test protocol, several pertinent measurement protocols for soot sampling from stationary sources were evaluated including the USEPA Engine Testing Procedures,⁴⁹ the USEPA Emissions Measurement Centre (EMC) Method 5 – Particulate Matter from stationary sources,⁵⁰ and the UNECE Vehicle Regulation No. 49.⁵¹

Although no specific guidelines existed for sampling from lab-scale flares, the consulted protocols were useful because they suggested general equipment and arrangements for the size of the DT, the DT flow rate measurement method, the sample probe type, the distance from the flow measurement and sample probe to the nearest disturbance, minimum DT flow rates, and conditions from the sample probe to the sampling device.

As shown in Table 3, the current system met or exceeded requirements from these three protocols, except where requirements of the different standards were contradictory, concerning dilution tunnel size and layout, dilution tunnel flow rate measurement, and sampling probe type and location. Ensuring that the exhaust gases were fully mixed within the DT was also critical. The fully mixed requirement was satisfied by ensuring that the Reynolds number in the DT was higher than 4000, and that the sample was sufficiently far downstream of any disturbances to ensure the exhaust gases were completely mixed. Good mixing was experimentally verified by traversing the DT with a probe to measure the soot volume fraction profile for both minimum and maximum expected DT flow rates.

When comparing sampling conditions among the cited sampling protocols, it became evident that all protocols controlled the temperature upstream of the sampling device (typically a filter assembly) as opposed to controlling the dilution ratio ($DR = Q_{Dilution\ Air} / Q_{Products}$). A protocol was therefore developed based on monitoring and controlling the temperature upstream of the measurement device as opposed to specifying a fixed dilution ratio or dilution ratio range, as further discussed below under the heading “Sampling Protocol”. This led to the use of a secondary dilution device that added filtered room temperature air upstream of the soot measurement device (as shown in Figure 3)

to cool the exhaust gases when specifically required. The three referenced protocols all suggested a different upstream temperature, so

the median value of $52\pm 5^\circ\text{C}$ was chosen for the current protocol.

Table 3: Comparison of sampling protocols

	Current Setup	USEPA ETP ⁴⁹	UNECE Reg. 49 ⁵¹	USEPA EMC ⁵⁰
Intended application	Lab-scale flares	PM from engines	PM from heavy vehicles	PM from stationary sources
DT diameter	6"	Not specified	>8"	4-12"
Flow measurement	Pitot rake, 17 measurements	Critical flow venturi, PDP, subsonic venturi, ultrasonic flow meter	Critical flow venturi, PDP	Standard Pitot tube
Sample inlet	Pitot tube, 1/4", upstream facing	Upstream facing probe	Upstream facing probe	Elbow or button hook (1/8 - 1/2")
Disturbance to flow measurement	21.2 diameters	>10 diameters	Not specified	>16 diameters
Disturbance to sample inlet	24.47 diameters	Not specified	>10 diameters	>8 diameters
DT flow rates	Min <i>Re</i> of 10,000	Min <i>Re</i> of 4,000	Min <i>Re</i> of 4,000	Not specified
Temperature upstream of filter	<52°C (maintained within $\pm 5^\circ\text{C}$)	$47 \pm 5^\circ\text{C}$	<52°C (maintained within $\pm 3^\circ\text{C}$)	$120 \pm 14^\circ\text{C}$
Iso-kinetic conditions?	No	Approximate	Yes	Within 10%
Sample device distance from sample port	0.5 m, insulated	As close as possible, insulated	<1.0 m	Immediate

Soot Sampling System

Two different measurement devices were used to measure the soot volume fraction in the sample gas stream as highlighted in Figure 3: a gravimetric sampling system and a laser induced incandescence (LII) instrument. The gravimetric system used 47 mm Millipore Fluoropore PTFE membrane filters (FGLP04700). Filter handling procedures (i.e. clean room temperature and humidity settings, filter charge neutralization, filter weighing procedures) were completed according to EPA TP 714C⁵² to determine the mass of soot collected, and when combined with the volume of sample gas drawn through the filter face and a soot density,⁴⁷ the soot volume fraction (f_v) could be found.⁵³ LII is a laser-based technique used to determine soot volume fraction in real-time. The reader is referred to Snelling et al.⁵⁴

for a detailed description of the theory behind its operation. The LII instrument used in the current work provided real-time measurements of f_v at a sample rate of 20 Hz. With either measurement technique, the resultant f_v values were combined with other measured parameters defined in eq 5 to produce the soot yield, Y_s , defined as the mass of soot produced per mass of fuel burned.⁵³

$$Y_s = \frac{\rho_{soot} f_{v,sample} Q_{DT} T_{sample}}{\dot{m}_{fuel} T_{DT}} \quad (5)$$

where ρ_{soot} is the soot density [kg/m^3], $f_{v,sample}$ is the soot volume fraction at the sample location measured by either technique, Q_{DT} is the dilution tunnel flow rate [m^3/s], T_{sample} is the gas temperature at the sample location [K], T_{DT} is the gas temperature in the dilution tunnel [K], and \dot{m}_{fuel} is the fuel mass flow rate [kg/s]. The

temperature ratio is necessary to correct the sample location soot volume fraction to the DT condition soot volume fraction. It is noted that eq 5 implicitly assumes that all soot was generated from the flare (as verified by a lack of detectable soot particles when tests were run without igniting the flame).

Sampling Protocol

A standard protocol was developed to ensure repeatable results. Of specific importance were the warm-up time, DT conditions, and sampling duration. The warm-up time was determined by monitoring several different temperature measurements on start-up, including the gas temperatures at the burner exit, inside the enclosure, in the DT, and upstream of the filter or heated sampling line. Once these temperatures reached stable values (generally around ~30 minutes), testing would commence.

The fan speed was then fine-tuned to regulate the sample temperature directly upstream of the filter by increasing or decreasing the amount of primary dilution air, in line with the protocol discussed above. If the primary dilution air alone was insufficient to cool the exhaust gases to the desired temperature, the secondary dilution device was activated to add a controlled amount of filtered building air to the sample. Although control of the exhaust gas temperature was not deemed necessary for LII operation, it was decided that conditions for measurements should be identical between gravimetric and LII tests.

Iso-kinetic sampling was not required in the present experiments due to the small size of the soot particles, as verified in three ways. Firstly, calculations using scanning mobility particle sizing (SMPS) data extracted from directly above the flame, showed that Stokes numbers of the soot aggregates were less than 0.01 for all conditions found in the experiments. At these low Stokes numbers, the particles track the flow

very efficiently, and fully representative samples would be collected even if the mismatch between the main flow and sample probe velocities was an order of magnitude or greater⁵⁵. Secondly, during the design of the experiment, the sampling system was sized so that the sampling duct to sample probe velocity ratio would fall as closely as possible to unity, and near isokinetic sampling would be achieved over the majority of operating conditions (never falling outside the range of 40-110% of the isokinetic sampling velocity). Thirdly, specific verification experiments were performed in which the direction of the sample probe within the sampling duct was rotated 180° to face away from the flow. Even under this extreme anisokinetic condition, samples matched those collected with the probe correctly positioned, which experimentally verified the prediction from the Stokes number calculations.

Although the reviewed sampling protocols all specified sample temperatures rather than dilution ratios, it is noted that some authors^{44,47,48} have cited dilution ratio as a parameter which can affect both the particle size, as well as the measured soot volume fraction. To ensure that the current sampling protocol was appropriate, and specifically to ensure that the dilution ratio in the sampling tunnel did not affect the measurements so long as the constant sample temperature condition was met, several tests were carried out using the 25.4 mm burner at 0.5 m/s burning the average 6-component fuel mixture. The fan speed was varied from 20-100% while the temperature upstream of the sample location was held to <52°C using the secondary dilution device when necessary. The results of these tests for both gravimetric and LII results showed negligible differences in the measured soot mass emission rate at the different fan speeds used, establishing the robustness of the current protocol. This is consistent with the conclusions of Ouf et al.⁴⁴, who in their study of over-ventilated diffusions

flames showed that the global equivalence ratio does not play a predominant role in the global mass production of soot particles emissions. Furthermore, during these tests the sample flow rate changed based on the amount of secondary dilution added, and the consistency of results was a further experimental verification that isokinetic sampling was not necessary in the present case, since the change in the strength of the sink (the sample probe) in the DT did not affect the measured soot yield.

The sampling duration for gravimetric tests was based on the minimum amount of sample required to ensure reasonable uncertainties. It was determined that a minimum of 50 μg of soot should be obtained for each filter test to ensure reasonable uncertainties ($< \sim 15\%$). By basing the test time on the amount of soot required, this meant that the test time could vary between five minutes for heavy sooting conditions to one hour for low sooting conditions. Test duration for the LII tests was determined via a convergence criterion applied to the time resolved data as it was recorded. The confidence interval (95% confidence level) of the test was calculated and a test was considered complete when this value was less than 0.5% of the mean, meaning that the calculated uncertainty and averaged measurement became stable.

During LII operation, anomalous soot volume fraction data points (1-2 orders of magnitude above the average) were occasionally observed. These erroneous data points resulted in large confidence intervals and were most likely due to large dust particles in the room air or possibly large soot particles deposited on the DT or sampling line walls being re-entrained into the flow. Chauvenet's criterion was used to filter these erroneous points from the soot volume fraction data output from the LII instrument. Chauvenet's criterion will discard a data point if the probability of obtaining the particular

deviation from the mean is less than $1/(2n)$, where n is the total number of sample points.

Uncertainty Analysis

A detailed uncertainty analysis was conducted based on the ANSI/ASME Measurement Uncertainty Standard,⁵⁶ which considers separate contributions of the systematic error (alternatively called bias error or instrument accuracy), denoted by B , and the precision error (or random error), denoted by P , to the total uncertainty (displayed in results figures as error bars). The standard assumes that the systematic uncertainties encountered are normally distributed. Each component error is estimated separately and then combined into a final uncertainty, U , in quadrature. The precision error is calculated by multiplying the standard error of the sample average by the appropriate 95% confidence interval t-value from the Student's t-distribution table as

$P = t_{\nu,95\%} \sigma / \sqrt{N}$, where σ is the sample standard deviation, N is the sample size, and the subscript ν is the degrees of freedom ($N-1$). The systematic and precision errors are assumed independent and combined in quadrature by the root sum of the squares method to produce an approximate total uncertainty, $U = \sqrt{B^2 + P^2}$.

The precision error is only calculated at the final stage of uncertainty analysis as it is assumed that the scatter in contributing components of the final uncertainty will be propagated to the scatter of the final calculated value. For example, if \bar{g} is an average of N measurements of g , and g is a function of x and y , each of which have an associated precision error, the final precision of \bar{g} is calculated as the scatter on g , where the precision error will reflect both precision errors within tests, and variation among tests.

RESULTS AND DISCUSSION

Soot yield values were determined using both measurement techniques for a large data set that

included multiple burner diameters, a range of fuel exit velocities, and different 4- and 6-component fuel mixtures. Results obtained using the two different approaches are plotted in Figure 4, which shows good linear correlation ($r^2=0.92$) within the calculated uncertainty limits displayed with error bars on the individual measurement points.

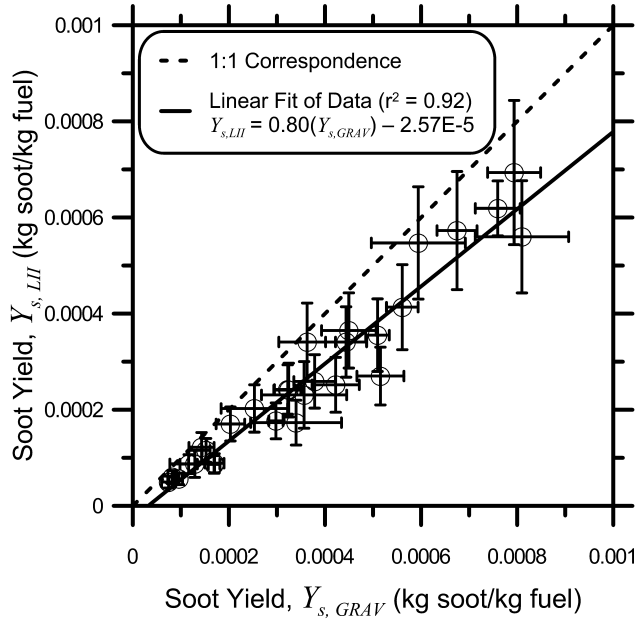


Figure 4: Comparison of LII and gravimetric measured soot yield.

The LII measured soot yield values are consistently lower than gravimetric measured soot yield values, which is expected since the LII technique heats the soot particles to temperatures approaching 4000 K, evaporating or sublimating all volatile components that may be condensed on the soot particles. Soot measured in this sense, i.e. by an optical absorption or emission based method, is commonly referred to as black carbon (BC), whereas the gravimetric values represent the total carbon. The difference between the two measurements is attributable to the organic

carbon (OC) fraction of the soot particles. The slope implies a mean black carbon to total carbon fraction of 0.80 in the emitted soot, although a measurement based on the NIOSH 5040 standard is likely to be better suited for accurately determining the relative carbon fractions in soot aggregates. Nevertheless, the agreement between these two techniques gives an important confidence in the measured results. Since the black carbon emissions are of particular interest in this work, only the LII recorded measurements will be discussed henceforth.

Scaling Soot Emissions

Several parameters cited in the literature^{37,40,41,47} were used in an attempt to scale soot emissions with flow conditions, including the fire Froude number, Fr_f ,³⁷ the Richardson ratio, Ri_L ,⁴⁰ the residence time, τ_R ,⁴¹ and a smoke-point normalized soot generation efficiency, SGE_{sp} .⁴⁷ Of these, the fire Froude number suggested by Delichatsios³⁷ proved the most effective. The Fr_f is similar to the fuel gas Froude number defined in eq 1, but includes an extra temperature ratio to account for flow acceleration due to buoyant forces produced in the flame, as defined in eq 6.

$$Fr_f = \frac{u_e f_s^{3/2}}{\left(\frac{\Delta T_f}{T_\infty} g d_e\right)^{1/2} \left(\frac{\rho_e}{\rho_\infty}\right)^{1/4}} \quad (6)$$

where ΔT_f is the characteristic temperature rise from combustion, typically calculated as the adiabatic flame temperature minus the ambient temperature [K], and T_∞ is the ambient temperature [K]. Soot yield is plotted as a function of the fire Froude number in Figure 5 for the average-mix 6-component fuel.

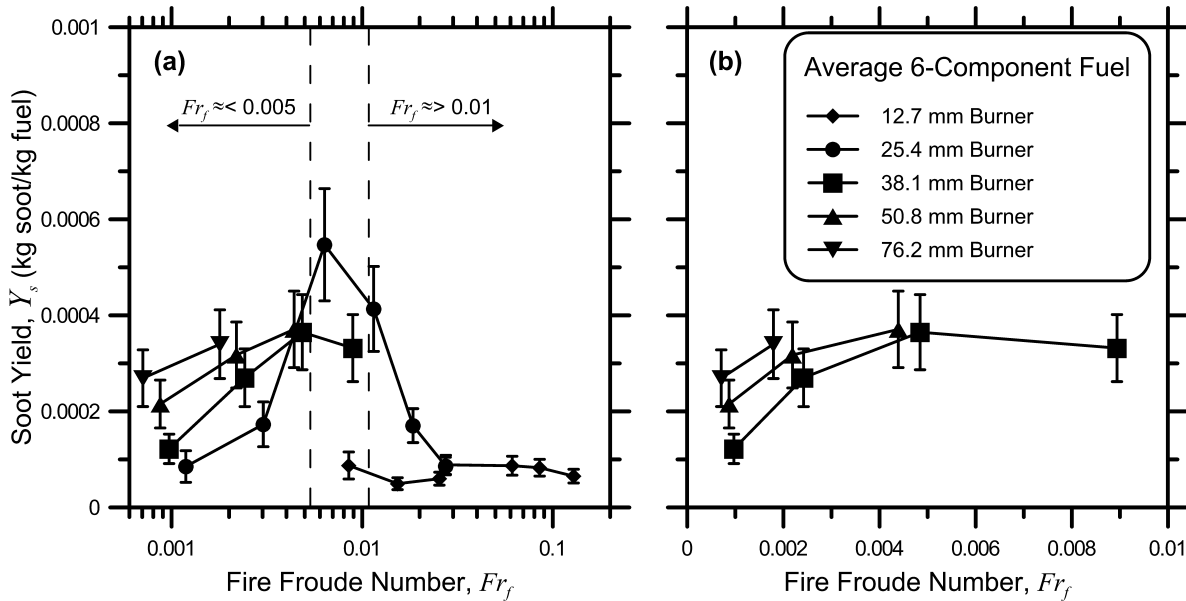


Figure 5: Soot yield as a function of the fire Froude number as defined by Delichatsios³⁷ for (a) all burners and (b) the three largest burners burning the average 6-component fuel. Dashed vertical lines represent the approximate transition region from “transition buoyant” to “transition shear” turbulent flames.

As apparent in Figure 5(a), there is no single trend among the data as a function of fire Froude number. However Figure 5(b), which plots only data from the three larger lab-scale flares (38.1, 50.8, 76.2 mm), illustrates that within this limited data set the data indicate a common trend: the soot yield appears to be increasing to a horizontally asymptotic value of ~ 0.0004 kg soot/kg fuel at a fire Froude number of ~ 0.005 for these three burners. Although the available data are quite limited, these results suggest there may be a transition in soot yield behaviour over the approximate range of $0.003 \leq Fr_f \leq 0.005$. While all of the tested flames would be classed as turbulent buoyant, this region closely correlates with the transition between the “transition buoyant” and “transition shear” regimes, as defined in the work of Delichatsios³⁷ and shown in Figure 1. Since the suggested transition line in Figure 1 is not vertical, the changeover between regimes occurs over a range of Froude numbers depending on the diameter and exit velocity. The approximate transition region for the current data set is indicated in Figure 5(a) as the area between the

vertical dashed lines. While the exact physical implications of this transition region are unclear, the data suggest that the different sub-regimes of turbulent buoyant flames do influence the soot yield, most notably for the 25.4 mm burner.

Further support for the observed behavior can be found in the work of Sivathanu and Faeth⁴¹ and Becker and Liang⁴⁰ who similarly noted a rise and plateau trend in their soot yield data (plotted in Sivathanu and Faeth in terms of a normalized residence time and in Becker and Liang in terms of the Richardson ratio and the characteristic residence time, defined as the first Damkohler number, all of which scale with Fr_f). The suggested trend in Figure 5(b) implies that if a typical 101.6 mm flare were operated at flow rates up to approximately 400 LPM, the soot yield would increase with increasing flow rate, and that above 400 LPM, the soot yield would remain reasonably constant.

Fuel Chemistry Effects

From the results discussed in Figure 5(b), it appears that flow effects on soot yield are minimized for Fr_f values greater than ~ 0.003 for the three largest burners (38.1, 50.8, 76.2 mm). A comparison of soot yields of these flares burning different fuel mixtures with $Fr_f \geq 0.003$ should thus highlight the effects of fuel chemistry alone. Two common parameters suggested in the literature^{39,43} for correlating fuel chemistry effects include the flame temperature and a smoke-point corrected heat release function; however neither of these parameters satisfactorily correlated the soot yield data presented here for different fuel mixtures.

Referring back to Table 1 where current soot emission factors were listed, the emission factor suggested by the CAPP guide³² was reported as a corrected version of a USEPA factor.²⁸ The correction was applied based on the volumetric heating value to a standard UOG associated gas heating value of 45 MJ/m^3 . In line with this notion, and recognizing that for the chosen range of similar fuel mixtures representative of associated gas composition found in the upstream oil and gas industry, the heating value is linearly correlated with the average carbon number of the fuel, the soot yield data were plotted as a function of the volumetric heating value, as shown in Figure 6.

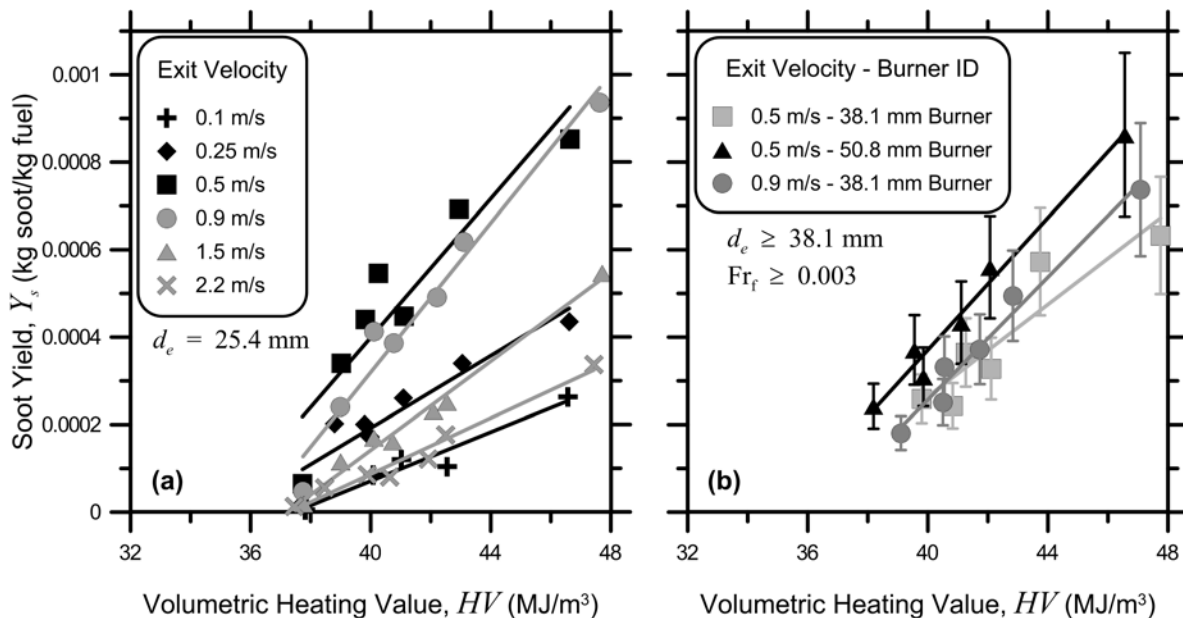


Figure 6: Soot yield as a function of the volumetric heating value for (a) the 25.4 mm burner and (b) values with a Fr_f greater than 0.003 and burner diameter of 38.1 mm or larger

Figure 6(a) shows that at any fixed flow condition, i.e. common burner diameter and exit velocity, a linear relationship exists between the measured soot yield and the fuel heating value (for the range of surrogate associated gas mixtures considered). However, at this burner size and low Fr_f values (< 0.003) the relative importance of fuel chemistry (heating value) in

determining the soot yield as compared to the influence of flow-related parameters, changes with the different flow conditions, as noted by the different slopes of Figure 6(a). In the regime of constant soot yield with flow condition (i.e. Fr_f greater than 0.003, burner diameter greater than 38.1 mm, Figure 6(b)), there is a strong linear correlation of soot yield with the

volumetric heating value. Notwithstanding the limited range of currently available data with which to test this correlation, the trend line fits well within the calculated uncertainty ranges of the individual measurement points. A correlation based on heating value makes physical sense, since both the volumetric heating value and the smoke-point increase with an increasing number of carbon atoms in the alkane-based fuel molecule (as well as alkene- and alkyne-based fuels).

Preliminary Emission Factors

As mentioned previously, a limit-scenario approach to soot yield measurements has been considered by ignoring crosswind effects. Consistent with this, we can neglect the effects of soot yield at fire Froude numbers less than 0.003, since the soot yield decreases at fire Froude numbers less than 0.003 for burner nozzle diameters of size 38.1 mm diameter or larger. Figure 7 displays the Emission Factor, EF , as a function of the heating value for burners of 38.1 mm, 50.8 mm, and 76.2 mm, at a range of flows where the fire Froude number is greater than 0.003 and includes data for all six fuel mixtures, which spans a range of gross heating values from $\sim 38 \text{ MJ/m}^3$ to $\sim 47 \text{ MJ/m}^3$. The correlation is reasonable ($r^2=0.85$), and the scatter of the data points is well within the uncertainty shown by the error bars (which indicate uncertainties of $<21\%$). While it must be stressed that there are not enough data to conclude that this trend will properly estimate soot emissions from flares of stack diameter up to 101.6 mm, the data are quite encouraging in the context of the literature review presented at the outset of this paper. Nevertheless, the reader is cautioned that because of the empirical nature of the correlation, it should be regarded as applicable only over the range of conditions tested experimentally.

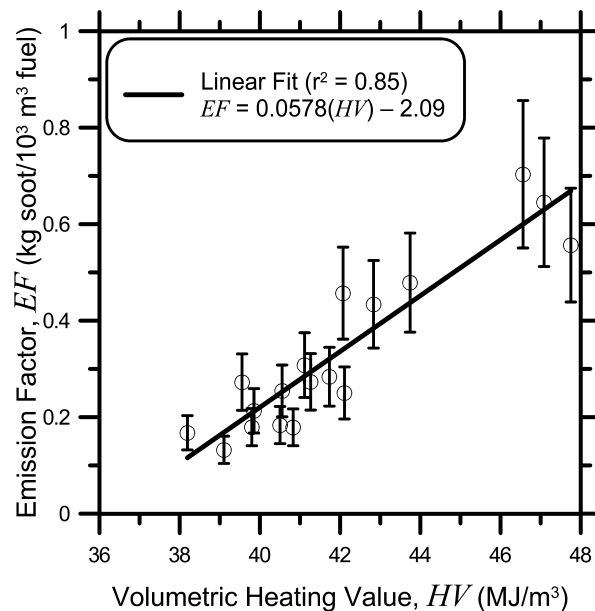


Figure 7: The Emission Factor as a function of the volumetric heating value for burners with diameters of 38.1 mm or larger and fire Froude numbers greater than or equal to 0.003

Comparing the current linear relationship for the present limited data set to the current CAPP Guide³² emission factor, a heating value of 45 MJ/m^3 would have an EF of approximately $0.51 \text{ kg soot}/10^3 \text{ m}^3 \text{ fuel}$ based on the current data, much less than the 2.5632 value currently suggested by CAPP³². Despite the limitations of the present data, given the origins of the current CAPP emission factor discussed previously, it seems the present model might still be more appropriate. The difference in these values could represent a significant difference for estimates of soot produced from burning associated gas. However, the range of conditions and fuels used must be expanded before the present relationship can be applied in regular industry practice with confidence.

SUMMARY

Total soot emissions from turbulent jet-diffusion flames representative of associated gas flares have been studied. Both a gravimetric sampling

method and a laser induced incandescence instrument were used in conjunction with a hood sampling system to measure the soot yield per mass of fuel burned for a wide range of conditions, including five different burner exit diameters, a broad range of flow rates, and six different fuel mixtures. A specific sampling protocol was developed for these measurements, based on current PM test protocols for stationary sources and diesel engines.

From the experiments, it was found that the soot yield behaved differently for the three largest burners (38.1 – 76.2 mm diameter) compared to the two smallest burners (12.7 and 25.4 mm diameter) and that the difference correlated with the transition between the “transition buoyant” and “transition shear” regimes, as defined in the work of Delichatsios.³⁷ Subsequent analysis focused on only the three largest burners, as these three exhibited similar behavior and were closer to the sizes of flares expected in the UOG industry. For these three largest burners, the limited available data suggested that soot yield values approached a constant value at fire Froude numbers greater than approximately 0.003, and below this value, the soot yield decreased with decreasing fire Froude number with different slopes for different burner diameters. This suggested trend has several potential implications, most notably that a flare designer or operator might affect the soot produced, if continuous flares (as opposed to emergency flares) are designed or controlled to operate with fire Froude numbers less than 0.003. If the data for fire Froude numbers greater than 0.003 are examined, the soot yield scales linearly with the fuel heating value, within this limited data set of flow rates and diameters, and for a range of mixtures relevant to associated gas compositions. A correlation based on heating value is justifiable in an engineering sense for its ease of application, because the heating value (like the smoke-point) increases with the number of carbon atoms in

the alkane-based fuel molecule, and typical gases flared in the UOG industry are methane dominated alkane mixtures.

Results from the currently available data suggest the emission factor for a fuel heating value of 45 MJ/m³ would be 0.51 kg soot/10³ m³ as opposed to the 2.5632 value currently suggested in the CAPP NPRI reporting guide,³² with the important caveat that this new value is based on limited data and should be used with caution. Nevertheless, the review presented in this paper suggests that the current CAPP factor may be even less reliable. For a very rough order of magnitude estimate, considering gas flared volumes of 139 billion m³/year as estimated from satellite data,¹ and estimating a single valued soot emission factor of 0.51 kg soot/10³ m³, flaring might produce 70.9 Gg of soot annually. This amounts to 1.6% of global BC emissions from energy related combustion, based on estimates of 4400 Gg for the year 2000.⁵⁷ It is also important to note that the current work is not attempting to suggest a single emission factor for estimating soot, but provides a preliminary empirical relationship between fuel heating value and soot yield. If fuel composition is known at a particular flare site, a specific emission factor based on the fuel could be used, which is an important improvement over the current single emission factor approach, especially considering the questionable origins of available emission factors as detailed in the paper.

ACKNOWLEDGEMENTS

This research was supported by Natural Resources Canada (Project Manager, Michael Layer), the Canadian Association of Petroleum Producers (CAPP), Environment Canada, National Research Council of Canada, and Carleton University. We are indebted to Pervez Canteenwalla, who constructed our original test facility during the course of his M.A.Sc. research. We are additionally grateful for the

input and insight of Kevin Thomson and Greg Smallwood of the National Research Council, Institute for Chemical Process & Environmental Technologies.

REFERENCES

1. Elvidge, C. D.; Ziskin, D.; Baugh, K. E.; Tuttle, B. T.; Ghosh, T.; Pack, D. W.; Erwin, E. H.; Zhizhin, M. A Fifteen Year Record of Global Natural Gas Flaring Derived from Satellite Data. *Energies* **2009**, *2*, 595-622; doi: 10.3390/en20300595.
2. IPCC Solomon, S.; Qin, D.; Manning, M.; Chen, Z.; Marquis, M.; Averyt, K. B.; Tignor, M.; Miller, H. L., Eds.; Cambridge University Press: Cambridge, UK and New York, USA, 2007; p. 996.
3. Strosher, M. T. Characterization of emissions from diffusion flare systems. *Journal of the Air & Waste Management Association* **2000**, *50*, 1723-33.
4. Pohl, J. H.; Lee, J.; Payne, R.; Tichenor, B. A. Combustion efficiency of flares. *Combustion Science and Technology* **1986**, *50*, 217-231.
5. Johnson, M. R.; Kostiuk, L. W. Efficiencies of low-momentum jet diffusion flames in crosswinds. *Combustion and Flame* **2000**, *123*, 189-200; doi: 10.1016/S0010-2180(00)00151-6.
6. Johnson, M. R.; Wilson, D. J.; Kostiuk, L. W. A fuel stripping mechanism for wake-stabilized jet diffusion flames in crossflow. *Combustion Science and Technology* **2001**, *169*, 155-174; doi: 10.1080/00102200108907844.
7. Pope III, C. A.; Burnett, R. T.; Thun, M. J.; Eugenia, E. C.; Krewski, D.; Ito, K.; Thruston, G. D. Lung Cancer, Cardiopulmonary Mortality, and Long-term Exposure to Fine Particulate Air Pollution. *JAMA: The Journal of the American Medical Association* **2002**, *287*, 1132-1141; doi: 10.1001/jama.287.9.1132.
8. US EPA *Integrated Science Assessment for Particulate Matter EPA/600/R-08/139F*; Washington, DC, 2010.
9. Hansen, J.; Sato, M.; Ruedy, R.; Lacis, A.; Oinas, V. Global warming in the twenty-first century: An alternative scenario. *Proceedings of the National Academy of Sciences of the United States of America* **2000**, *97*, 9875-9880.
10. Ramanathan, V.; Carmichael, G. Global and regional climate changes due to black carbon. *Nature Geoscience* **2008**, *1*, 221-227; doi: 10.1038/ngeo156.
11. Johnson, M. R.; Coderre, A. R. An Analysis of Flaring and Venting Activity in the Alberta Upstream Oil and Gas Industry. *Journal of the Air & Waste Management Association* **2011**, *61*, 190-200; doi: 10.3155/1047-3289.61.2.190.
12. Brzustowski, T. A. Flaring in the energy industry. *Progress in Energy and Combustion Science* **1976**, *2*, 129-141; doi: 10.1016/0360-1285(76)90009-5.
13. Johnson, M. R.; Kostiuk, L. W. A parametric model for the efficiency of a flare in crosswind. *Proceedings of the Combustion Institute* **2002**, *29*, 1943-1950; doi: 10.1016/S1540-7489(02)80236-X.
14. Kostiuk, L. W.; Majeski, A. J.; Poudenx, P.; Johnson, M. R.; Wilson, D. J. Scaling of wake-stabilized jet diffusion flames in a transverse air stream. *Proceedings of the Combustion Institute* **2000**, *28*, 553-559; doi: 10.1016/S0082-0784(00)80255-6.
15. Kostiuk, L. W.; Johnson, M. R.; Thomas, G. *University of Alberta Flare Research Project Final Report*; Edmonton, 2004; p. 254.
16. Pohl, J. H.; Soelberg, N. R. *Evaluation of the efficiency of industrial flares: Flare head design and gas composition*; United States Environmental Protection Agency: Research Triangle Park, NC, 1985; p. 140.
17. Siegel, K. D. Degree of conversion of flare gas in refinery high flares. Ph.D. Thesis, Fridericiana University Karlsruhe, Germany, 1980, p. 192.
18. Strosher, M. T. *Investigation of Flare Gas Emissions in Alberta*; Calgary, Alberta, 1996.
19. Poudenx, P. Plume sampling of a flare in crosswind: structure and combustion efficiency, University of Alberta, Edmonton, AB, Canada: Edmonton, 2000, p. 173.
20. Howell, L. Flare stack diameter scaling and wind tunnel ceiling and floor effects on model flares, University of Alberta, Edmonton, AB, Canada, 2004, p. 185.
21. Bourguignon, E.; Johnson, M. R.; Kostiuk, L. W. The use of a closed-loop wind tunnel for measuring the combustion efficiency of flames in

- a cross flow. *Combustion and Flame* **1999**, *119*, 319-334; doi: 10.1016/S0010-2180(99)00068-1.
22. Johnson, M. R.; Kostink, L. W. In *IUTAM Symposium on Turbulent Mixing and Combustion*; Pollard, A.; Candel, S., Eds.; Kluwer Academic Publishers: Kingston, ON, 2002; Vol. 70, pp. 295-303.
 23. ERCB Directive 060: Upstream Petroleum Industry Flaring, Incinerating, and Venting **2006**.
 24. McDaniel, M. *Flare efficiency study*; United States Environmental Protection Agency: Research Triangle Park, NC, 1983; p. 133.
 25. Johnson, M. R.; Devillers, R. W.; Yang, C.; Thomson, K. A. Sky-Scattered Solar Radiation Based Plume Transmissivity Measurement to Quantify Soot Emissions from Flares. *Environmental Science & Technology* **2010**, *44*, 8196-8202; doi: 10.1021/es1024838.
 26. Johnson, M. R.; Devillers, R. W.; Thomson, K. A. Quantitative Field Measurement of Soot Emission from a Large Gas Flare Using Sky-LOSA. *Environmental Science & Technology* **2011**, *45*, 345-50; doi: 10.1021/es102230y.
 27. Ellzey, J. L.; Berbe, J. G.; Tay, E. Z. F.; Foster, D. E. Total Soot Yield from a Propane Diffusion Flame in Cross-Flow. *Combustion Science and Technology* **1990**, *71*, 41-52.
 28. US EPA WebFIRE (Factor Information REtrieval System) v.6.25. v.6.25 **2009**.
 29. US EPA *Data from flaring landfill gas, Confidential Report*; 1991.
 30. US EPA AP-42 - *Compilation of Air Pollutant Emission Factors, Volume I, 5th ed. - Section 2.4*; Research Triangle Park, NC, 1998; pp. 1-19.
 31. US EPA AP-42 - *Compilation of Air Pollutant Emission Factors, Volume I, 5th ed. - Section 13.5*; Research Triangle Park, NC, 1995.
 32. CAPP *A Recommended Approach to Completing the National Pollutant Release Inventory (NPRI) for the Upstream Oil and Gas Industry*; 2007; pp. 1-146.
 33. Huang, R. F.; Wang, S. M. Characteristic flow modes of wake-stabilized jet flames in a transverse air stream. *Combustion and Flame* **1999**, *117*, 59-77; doi: 10.1016/S0010-2180(98)00070-4.
 34. Gollahalli, S. R.; Nanjundappa, B. Burner Wake Stabilized Gas Jet Flames in Cross-Flow. *Combustion Science and Technology* **1995**, *109*, 327-346; doi: 10.1080/00102209508951908.
 35. Becker, H. A.; Liang, D. Visible Length of Vertical Free Turbulent Diffusion Flames. *Combustion and Flame* **1978**, *32*, 115-137.
 36. Peters, N.; Göttgens, J. Scaling of Buoyant Turbulent Jet Diffusion Flames. *Combustion and Flame* **1991**, *85*, 206-214.
 37. Delichatsios, M. A. Transition from momentum to buoyancy-controlled turbulent jet diffusion flames and flame height relationships. *Combustion and Flame* **1993**, *92*, 349-364; doi: 10.1016/0010-2180(93)90148-V.
 38. Johnson, M. R.; Kostiuk, L. W.; Spangelo, J. L. A characterization of solution gas flaring in Alberta. *Journal of the Air & Waste Management Association* **2001**, *51*, 1167-1177.
 39. Delichatsios, M. A. Smoke yields from turbulent buoyant jet flames. *Fire Safety Journal* **1993**, *20*, 299-311.
 40. Becker, H. A.; Liang, D. Total emission of soot and thermal radiation by free turbulent diffusion flames. *Combustion and Flame* **1982**, *44*, 305-318.
 41. Sivathanu, Y. R.; Faeth, G. M. Soot volume fractions in the overfire region of turbulent diffusion flames. *Combustion and Flame* **1990**, *81*, 133-149; doi: 10.1016/0010-2180(90)90060-5.
 42. Turns, S. R. *An Introduction to Combustion: Concepts and Applications*; 2nd ed.; McGraw-Hill: USA, 2000.
 43. Glassman, I. Sooting laminar diffusion flames: Effect of dilution, additives, pressure, and microgravity. *Proceedings of the Combustion Institute* **1998**, *27*, 1589-1596.
 44. Ouf, F.-X.; Vendel, J.; Coppalle, A.; Weill, M.; Yon, J. Characterization of Soot Particles in the Plumes of Over-Ventilated Diffusion Flames. *Combustion Science and Technology* **2008**, *180*, 674-698; doi: 10.1080/00102200701839154.
 45. Kostiuk, L. W.; Thomas, G. P. *Characterization of Gases and Liquids Flared at Battery Sites in the Western Canadian Sedimentary Basin*; Edmonton, 2004; p. 95 pages.
 46. Smith, C. R.; Tracy, G. W.; Farrar, R. L. *Applied Reservoir Engineering, Vol. 1*; Oil & Gas

- Consultants International: Tulsa, OK, 1992; pp. 3-2 - 3-3.
47. Canteenwalla, P. M. Soot emissions from turbulent diffusion flames burning simple alkane fuels, Carleton University, Ottawa, ON, Canada, 2007, p. 159.
 48. US EPA 40 CFR Part 1065 Engine-Testing Procedures. *Federal Register* **2005**, *70*, 40516-40612.
 49. US EPA 40 CFR Part 60 Test Method 5 - Determination of Particulate Matter Emissions from Stationary Sources **2000**, 371-442.
 50. UNECE *Regulation No. 49 - Uniform Provisions Concerning the Measures to be Taken Against the Emissions of Gaseous and Particulate Pollutants from Compression-Ignition Engines for Use in Vehicles, and the Emission of Gaseous Pollutants from Positive-Ignition Eng*; 2008; pp. 1-520.
 51. US EPA *TP 714C - Diesel particulate filter handling and weighing*; 1994.
 52. McEwen, J. D. N. Soot Emission Factors from Lab-Scale Flares Burning Solution Gas Mixtures. M.A.Sc. Thesis, Carleton University, Ottawa, ON, Canada, 2010, p. 146.
 53. Snelling, D. R.; Smallwood, G. J.; Liu, F.; Gülder, Ö. L.; Bachalo, W. D. A calibration-independent laser-induced incandescence technique for soot measurement by detecting absolute light intensity. *Applied Optics* **2005**, *44*, 6773-6785; doi: 10.1364/AO.44.006773.
 54. Chang, M. C.; Chow, J. C.; Watson, J. G.; Hopke, P. K.; Yi, S. M.; England, G. C. Measurement of Ultrafine Particle Size Distributions from Coal-, Oil-, and Gas-Fired Stationary Combustion Sources. *Journal of the Air & Waste Management Association* **2004**, *54*, 1494-1505.
 55. Hinds, W.C. *Aerosol Technology: Properties, Behavior, and measurement of airborne particles* (2nd ed.), Wiley-Interscience, 1999.
 56. ANSI/ASME *ANSI/ASME PTC 19.1 - Part 1 – Measurement Uncertainty, Instruments and Apparatus*; 1985.
 57. Bond, T. C.; Bhardwaj, E.; Dong, R.; Jogani, R.; Jung, S.; Roden, C.; Streets, D. G.; Trautmann, N. M. Historical emissions of black and organic carbon aerosol from energy-related combustion, 1850–2000. *Global Biogeochemical Cycles* **2007**, *21*, 1-16.
 58. Eklund, B.; Anderson, E. P.; Walker, B. L.; Burrows, D. B. Characterization of Landfill Gas Composition at the Fresh Kills Municipal Solid-Waste Landfill. *Environmental Science & Technology* **1998**, *32*, 2233-2237.

ABOUT THE AUTHORS

James D.N. McEwen is a recent Master's graduate and research engineer with the Energy and Emissions Research Lab at Carleton University. Matthew R. Johnson is a Canada Research Chair in Energy & Combustion Generated Pollutant Emissions and an associate professor at Carleton University where he heads the Energy and Emissions Research Lab. Please address correspondence to: Matthew Johnson, Carleton University, Mechanical and Aerospace Engineering, 1125 Colonel by drive, Ottawa, ON, K1S 5B6; phone: +1-613-520-2600 x. 4039; fax: +1-613-520-5715; email: matthew_johnson@carleton.ca.